Modeling and Assessment of D-STATCOM in Grid Connected PV System Using ANN and ANFIS Controller

Ali AlQattan *‡, S. Ali Al-Mosawi **, Fadhel Albasri ***

*Department of Electrical Engineering, University of Bahrain, Student, Bahrain

**Department of Electrical Engineering, University of Bahrain, Associate Professor, Bahrain

***Department of Electrical Engineering, University of Bahrain, Assistant Professor, Bahrain

(aliqwert30@hotmail.com, aalmossawi@uob.edu.bh, falbasri@uob.edu.bh)

‡Corresponding Author; Ali AlQattan, Department of Electrical Engineering, University of Bahrain, Student, Bahrain, Tel: +973-33951989, aliqwert30@hotmail.com

Received: 17.11.2023 Accepted:06.01.2024

Abstract- Photovoltaic (PV) solar energy is regarded as one of the most abundant forms of renewable energy. As a result, more PV systems are being installed, which is leading to new power quality issues in grid systems. Unbalanced voltages, changing power levels, harmonic distortions, or reverse power flow are a few instances of these issues. Distribution Static Synchronous Compensation (D-STATCOM) is viewed as a potential remedy to lessen the negative effects of PV integration on voltage regulation and harmonic distortion in electrical distribution systems. By developing and contrasting an enhanced control system for D-STATCOM. By simulating a power system model with an integrated PV system and D-STATCOM, simulation research is carried out. To improve the power quality of the power system, two control schemes Artificial Neural Network (ANN), and Adaptive Neuro-fuzzy Inference System (ANFIS) were implemented within the internal control of D-STATCOM. A Hysteresis Current Controller and a Sinusoidal Pulse Width Modulation (SPWM) inverter arrangement were modified (HCC). Results are produced in the form of voltage profiles for all the control schemes taken into consideration with various inverter types under various contingency scenarios. Control characteristic evaluation for various controllers is another method used to assess performance. Graphical techniques, Total Harmonic Distortion (THD), and Root Mean Squared Error were used to examine various scenarios (RMSE). This work has made the following original contributions to the area of D-STATCOM systems where, different controller techniques and inverter are applied to D-STATCOM and compared to find out the best type of control. The result proven that the performance of SPWM with ANFIS was better than other control schemes in most of the scenarios. Hence, it was found that the SPWM inverter strategy adapts the control input fast rather than the Hysteresis scheme. The above conclusion signifies that the performance of advanced controllers, especially ANFIS, was best among other controllers. It can effectively be used to enhance the power quality of the power system using D-STATCOM devices.

Keywords D-STATCOM, power quality, harmonics, total harmonic distortion.

1. Introduction

The massive increase in power demand brought on by loads in the residential, commercial, and agricultural sectors has a considerable impact on energy consumption [1]. Electricity producers, users, and grid operators are all impacted by power quality. Deviations from the ideal waveforms of voltage and current are the main problems with power quality. Long-duration voltage fluctuations (sustained voltage oscillation and under voltage), oscillatory and spontaneous transients, voltage flicker, short-duration voltage fluctuations (dip or sag, interruption, and swell) as shown in “Fig. 1”, waveform distortion (DC offset, notching, and harmonics), & voltage imbalance are a few examples of

power quality concerns. Natural disasters, distribution or transmission, distribution breakdowns, and electricity consumers typically make these issues worse.

Voltage fluctuations can have undesirable effects, such as making lighting equipment flicker. Voltage sag can cause surges and overloading problems in electronic systems, which can result in intermittent lockup. On the other hand, voltage swell can damage electrical machinery, Transformers, motors, and other electrical machinery are all susceptible to harm from harmonics.

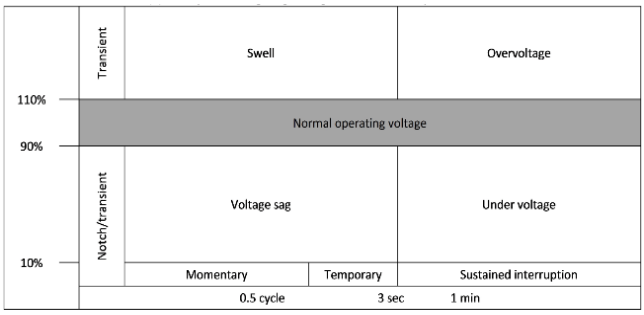

Fig. 1. Classification of voltage sag and swell [2].

Due to the global energy crisis and environmental pollution caused by conventional energy sources, solar photovoltaic (PV) now a day consider of most common renewable energy is used, and it is becoming more widespread across the globe [3]. As a result, it is quickly incorporated into power systems, and the installed capacity of PV systems is increasing, which mainly use power electronic controllers cause increased power quality problems [4]. Output power of PV with varying climate conditions can be unpredictable as it can fluctuate throughout the day [5]. As a result, new power quality issues for grid systems have emerged, including low inertia, imbalanced voltage or fluctuating power levels, harmonic distortion, and reverse power flow [2]. Power quality difficulties include voltage and frequency variation, voltage sag, voltage surge, harmonics, reverse power flow, synchronization problems, and intermittent power flow are serious obstacles to the integration of PV power into the grid [6].

1.1 Motivation

The intermittent nature of PV energy sources contributes to voltage fluctuation on the grid, which may get worse as PV adoption increases [7]. Integration of PV power into the grid presents severe power quality challenges such as voltage and frequency variation; voltage sag; voltage surge; harmonics; reverse power flow; synchronization issues; and intermittent power flow, when a voltage profile deviates from the IEEE-defined limit and the amplitude of a voltage fluctuation is consistent and stays within the bounds specified by ANSI C84.1 and IEEE standard 1250-1995, there is a voltage fluctuation. The nominal value's variations typically range from 0.9 to 1.1 percent.

Another significant issue resulting from the increased penetration of PV energy sources is a harmonic distortion of current and voltage. The voltage or current harmonics are sinusoidal waveforms whose frequencies are integer multiples of fundamental frequencies, resulting in a distorted waveform. It occurs in a PV energy system due to power electronic components such as an inverter that converts the dc output of photovoltaic panels to alternating current signals, according to IEEE standard 519 -1992, each specific harmonic distortion cannot be greater than 3%, and the Total Harmonic Distortion (THD) rate must be less than 5% of the fundamental frequency [8]. If the THD is higher than the threshold, there is a serious power quality risk. Such systems do not comply with international norms [8]. As a result of the damage done to its fragile components, the lifespan of electronic equipment is decreased [9].

The control of active power injection/absorption is the best solution for the power oscillation damping and can improve the transient stability. D-STATCOM is the most dominant technology for power quality and harmonic power mitigation in distribution networks. Typically, the D-STATCOM is based on the voltage source converter [10]. D-STATCOM compensator can provide reactive power compensation and harmonic filtering [11]. A D-STATCOM with an energy storage system can control both the reactive and the active power injection/absorption, thus providing a more flexible power system operation. In a nutshell, D-STATCOM became an advantageous solution for several problems that are being faced by both electric utilities as well as industries. Its advantages could be summarized as follow:

- It is essential to keep voltage levels in a safe range.
- Improvement of the transient stability of the power system through reactive and active regulation of the system's output.
- Increased power transfer capability.
- Reduction of the power oscillations.
- Unsymmetrical load balancing.
- Reduction of transmission line losses.

2. Literature Review

To handle power quality (PQ) problems on the distribution side, the Distribution Static Synchronous Compensator (D-STATCOM) is implemented dynamically. The distribution compensator outperforms all other controllers on the market when it comes to addressing poor power quality. The performance of conventional distribution methods has decreased as electrical power usage has grown quickly. D-STATCOM was used to create better compensated strategies as a result [12].

Different algorithms have been presented in the literature, including carrier-based algorithms such as Synchronous

Reference Frame (SRF) [13], [14], carrier-fewer algorithms [15], and Power Balanced Theory (PBT) [16], fuzzy-PI based CSI control algorithm [17].

The use of artificial intelligence for renewable energy sources has increased, especially for Solar. The application of AI for renewable and energy sources offers interesting characteristics, such as independent learning, and large-scale decision-making [18].

The sinusoidal pulse width modulation (SPWM) approach D-STATCOM also uses a PI controller to sustain a stable voltage across a capacitor via a DC link capacitor, to some extent, the PI controller works well and provides superior results, but dynamic and highly nonlinear loads hinder the system's stability [19].

2.1 Study Significance and literature gap

This study work has made the following original contributions to the area of D-STATCOM systems:

- Different controller techniques are applied to D-STATCOM and compared to achieve the best results, by investigating different controllers for D-STATCOM such ANN and ANFIS, as well as different inverter types of SPWM and HCC. The results of this investigation would reveal the best kind of controller that will be proposed. This investigation will be carried out by developing the proposed controllers in MATLAB.
- The results are obtained as voltage profiles for all control schemes under different operating and fault scenarios. Further performance evaluation was performed by evaluating the control characteristics of different controllers in MATLAB/SIMULINK with different scenarios. In addition, analyzing all control schemes using total harmonic distortion (THD).
- All results obtained are as voltage profiles for all control schemes under different scenarios. Further performance evaluation done by applying the control characteristics evaluated by calculating Root Mean Square Error (RMSE), Steady State Error, Settling Time, Settling Average value, Rise time, and the peak value to explore an in-depth analysis of each controller type.

3. System Model and Configuration

A distributed static compensator (D-STATCOM) configuration with a load for a three-wire 3-ϕ distribution system is illustrated in "Fig. 2". Using 3-ϕ transformers with voltage ratings of 11/0.415 kV, a 3-ϕ load can be connected to a 3-ϕ source voltage of 415V. The D-STATCOM is connected to the PCC for the harmonic's reduction and regulation of voltages at the bus interface.

The two main parts of D-STATCOM are the controller and a voltage source converter (VSC). A power system can produce a changeable AC voltage source by using a voltage source inverter and a DC capacitor as the input to a D-STATCOM. When a voltage differential is applied across this reactance to form the D-STATCOM, an active and reactive power transfer happens. To address problems with voltage quality, the D-STATCOM is connected to networks inside the power system. A three-wire 3- distribution system using a distributed static compensator (D-STATCOM) Configuration with a load. An electrical connection between a 3-load and a 3-source voltage of 415V can be made using 3-transformers with voltage ratings of 11/0.415 kV. To reduce harmonics and regulate voltages at the bus interface, the D-STATCOM is linked to the PCC as shown in "Fig. 3".

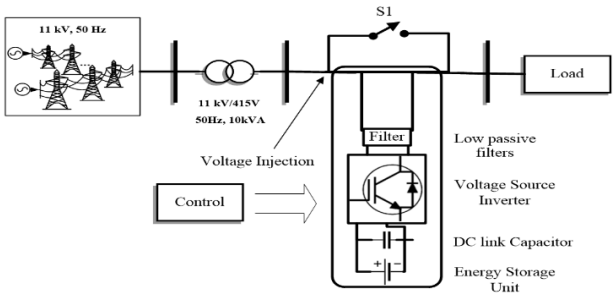

Fig. 2. D-STATCOM configuration.

This simulation model was chosen because it combines the study goal and domain to provide an accurate simulation that will explain the effects of various controllers. A step-down transformer with an 11 kV, 50 Hz voltage rating is used in a typical distribution system to supply the various load types.

The voltage of the distribution line to the consumer is 415V, which is Bahrain's standard rating. Under various load conditions, VSI-based D-STATCOM switching is employed for voltage compensation, and the controller acquires the fundamental reference control signals for switching. The D-STATCOM Simulink model was utilized in the study work to create the suggested strategy and execute simulations.

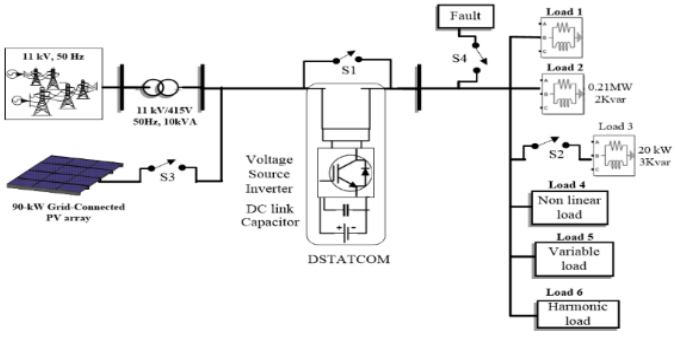

Fig. 3. Single line diagram of the proposed test system for this research.

4. D-STATCOM Regulation Controller in MATLAB

frame theory-based control was used to create switching pulses for the three-phase D-STATCOM. In three-phase system, the 3-ϕ (in abc frame) currents or voltages are transformed to a stationary $\alpha - \beta$ frame and subsequently to a D-Q spinning frame.

Thus, at least two phases are required to convert a signal to a stationary $\alpha - \beta$ frame. The α-axis components are represented by the original signal, whereas the stationary reference component is β -axis frame and lags by 90o. Input signals such as the voltages at the PCC (Va, Vb, Vc), and the voltages at the dc bus (Vdc) and the load current (il), are all monitored and used as signal to the system. Using balanced and sinusoidal PCC voltages, the system voltage amplitude is computed as [19].

It is essential to the functionality and quality of D-STATCOM to create the compensating reference current. The voltage regulation controller in the dc-link is a crucial component. The dc-link voltage (v dc) can be altered in one of two ways to account for compensating current: either option is acceptable. To ensure effective VSI operation, a certain reference value on the inverter's dc side is necessary. Keeping the dc-link voltage constant lessens VSI switching. The mean active current factor (i (D dc)) must be applied to the dc-link voltage to maintain stability according to the rotating frame theory.

To improve the effectiveness of the D-STATCOM under normal operating conditions and during contingencies, an ANN and ANFIS controller was applied instead of the existing PI controller in the D-STATCOM controller.

First, Artificial Neural Networks (ANNs), which are adaptive techniques with incredible information-processing capabilities, comprise layers of neural nodes that communicate with one another. It is desired for artificial neural models to have certain qualities for the following reasons: (a) better data fit is made possible by nonlinearity, (b) in the presence of unclear data and measurement errors, noise insensitivity leads to accurate forecasting, (c) with more parallelism comes increased speed, and greater hardware fault tolerance, (d) learning and adaptability make it possible for the system to respond to changes in its surroundings by changing its internal structure and (e) the model can be applied to previously unrecognized data through generalization [20].

Second, Adaptive Neuro-Fuzzy Inference System (ANFIS) combines the ability of ANN to learn and its relational structure with the ability of fuzzy logic to make decisions. As with ANN, ANFIS uses samples to learn from a training data set. Therefore, the optimal ANFIS structure for handling the relevant issue is discovered. The resulting structure is put through its paces to assess how it performs with samples that have never been encountered before. The ANFIS model's lower error rates prove its suitability. In an artificial

The single-phase synchronous D-Q frame theory-based control technique for the three-phase D-STATCOM. A D-Q

neural network, the weight values cannot be justified, as the inability to explain the value of the weights belonging to an ANN model is a disadvantage. Due to this significant problem, the ANFIS framework has a fuzzy inference technique that eliminates this drawback. Many real-world problems can be solved because of their structure [21].

The necessary training data set has been prepared from the system and consists of two input (error and integration of error) and one output of each PI controller. training data was collected by simulation. But with using only load-1 and load-2 and by connecting D-SATCOM from 1s to 12s. the PI controller parameter is calculated from equation (23), (24), (33) and (34) described in Section 3 and result is $K_{pd} = 0.014$, $K_{id} = 2$, $K_{pq} = 0.0041$ and $K_{iq} = 200$ where $R_{st} = 0.004$, $L_{st} = 0.003$ and by considering $\delta = 0.707$ [22], [23].

To improve the effectiveness of the D-STATCOM under normal operating conditions and during contingencies, an ANN and ANFIS controller was applied instead of the existing PI controller in the D-STATCOM controller.

5. Simulation Analysis

An electric distribution network system with an integrated renewable energy system is modelled and simulated in MATLAB/Simulink. “Fig. 3”. illustrates the simulated electrical system, which consists of a voltage source representing the grid with a 90kW solar PV array, a distribution transformer, a D-STATCOM, and six different loads as shown in “Table 1.”

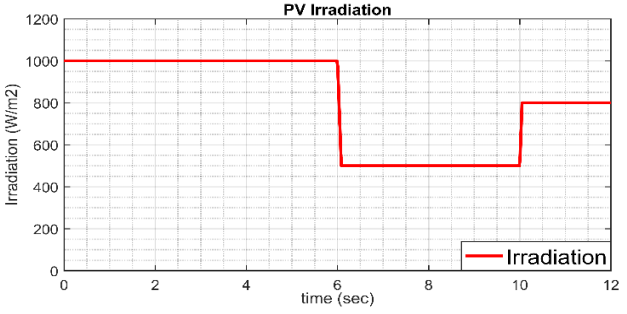

Fig. 5. Solar PV irradiance graph.

The power system that is connected to the PV system and D-STATCOM under various loading scenario as shown in “Table 2.” The simulations lasted 12 seconds. The six different types of loads are previously listed.

To regulate the load voltage profile under eight different operating scenarios for the power system, this compares the performance of six control schemes (SPWM-ANN, SPW-ANFIS, Hysteresis-ANN, and Hysteresis-ANFIS) with the load's overall RMS voltage signal is displayed in “Fig. 4” The PV system is activated at time 2.5s and deactivated at time 11s

for simulation purposes. The PV irradiation is changed with different irradiation values in order to simulate changes in irradiation and their effect on the grid network as shown in "Fig. 5". The solar irradiance of 1000 W/m2 is used from time 0 - 6 s, and then reduced to 500 W/m2 for t = 6 -10 s and then increased again to 800 W/m2. The change in solar irradiance is necessary to incorporate the intermittency of sunlight due to the diverse weather like sunny and overcast conditions.

Table 1. Different load types and parameters used in the simulation

Load Number	Active Time	Load Type	Parameters
Load 1	0-12s active	Fixed Impedance Load	Phase A: (15 Ω + j 11 Ω)
			Phase B: (30 Ω + j 15 Ω)
			Phase C: (60 Ω + j 65 Ω)
Load 2	0-12s active	Constant Active and Inductive power load	Active power 0.21 MW + inductive reactive power 2k VAR
Load 3	2-8s active	Constant Active and Inductive power load	Active pow. 20 kW + reactive pow. 3kVAR
Load 4	2-8s active	Non-linear load	200-ohm, 1×10^{-3} H , 600×10^{-6} F
Load 5	0-12s active	Variable load	7 Ω with a standard deviation ±1
Load 6	0-12s active	Non-linear (harmonic) load	150 Ω, 500×10^{-6} F

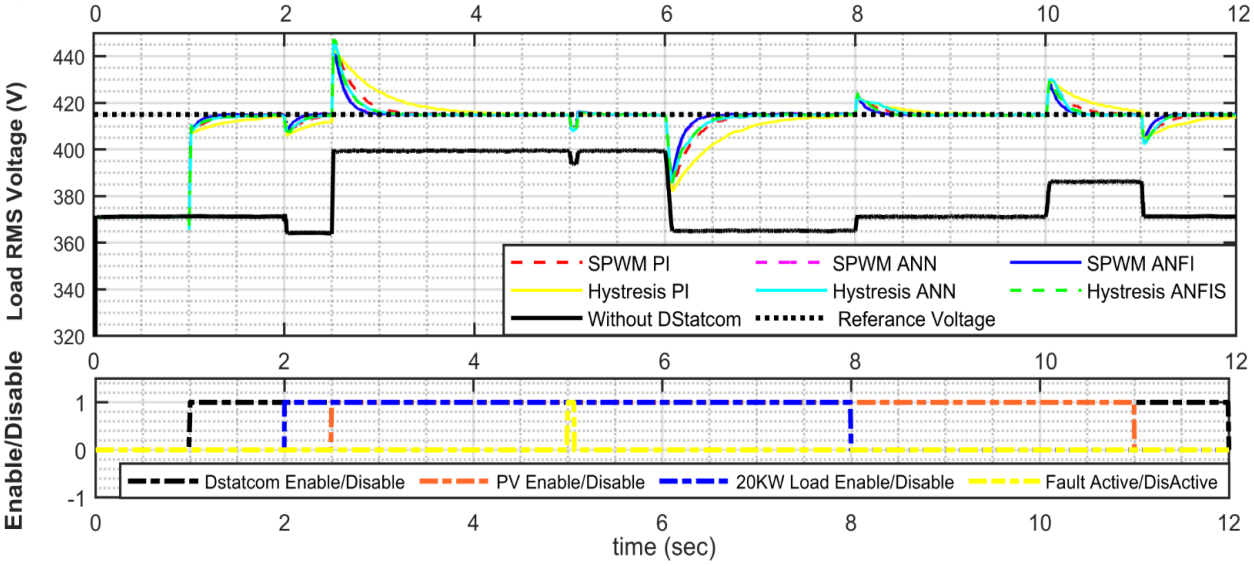

Fig. 4. Simulation result for 12s of simulation describes PV, RMS voltage, and the eight different operating scenarios.

Table 2. The eight different scenarios of simulation

Sr.	Scenarios	Seconds
1	D-STATCOM system connected	1
2	Load-3 and Load-4 active	2
3	PV connected to the grid with 100% capacity	2.5
4	ABG Fault active	5
5	PV drop to 50% capacity	6
6	Load-3 and Load-4 dis-active	8
7	PV increase to 80% capacity	10
8	PV dis-connected from the grid	11

6. Results and Discussion

The next sections will go into great depth about each voltage adjustment. By evaluating the settling time, settling average value, rise time, and peak value, together with the root mean square error (RMSE), steady state error (SS Error), and other voltage profile control parameters, this result is further analyzed quantitatively.

A. Scenario 1: D-STATCOM On

As soon as the D-STATCOM is enabled, the load RMS voltage is adjusted to the reference voltage (415V) as shown in "Fig. 6". The ANFIS controller using SPWM has the smallest RMSE, settling time, and rising time, as shown in "Table 3."

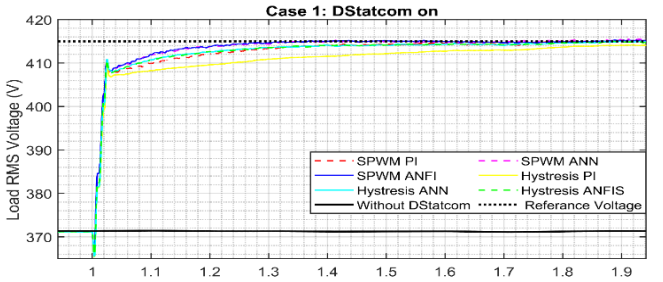

Fig. 6. RMS voltage while D-STATCOM active.

However, the best SSError and Settling Average Value are found in ANN controllers with SPWM. Additionally, the RMSE, settling time, and rising time are all the lowest with the ANFIS/ANN controller. This illustrates that the SPWM inverter outperforms the hysteresis inverter in terms of performance.

B. Scenario 2: Active, Reactive, and Non-Linear Load -On

As demonstrated in "Fig. 7', when an extra load is attached to the system, the D-STATCOM regulates the load RMS voltage to the reference voltage (415V). Additionally, it shows that the controller of ANFIS and ANN modulated by SPWM results in the quickest response time. Similarly, from "Table 4." the controller ANFIS with SPWM has the best Settling Average Value and the lowest RMSE, settling time, and rising time.

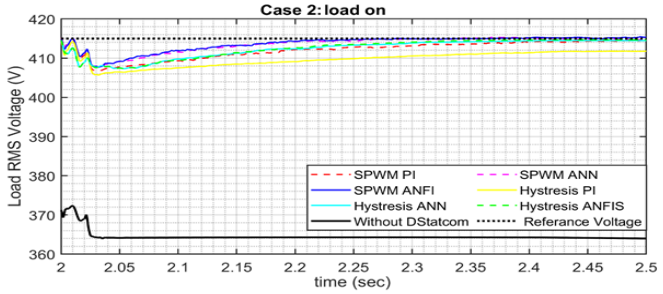

Fig. 7. RMS voltage of additional load active.

However, compared to the other controllers, the ANN controller utilizing SPWM has a lower SSError value. The settling time is the shortest for the SPWM ANFIS and Hysteresis ANFIS controllers, while the rise time is the shortest for the SPWM ANFIS and ANN controllers. It also shows how the SPWM inverter & hysteresis inverter works differently in this situation.

C. Scenario 3: PV on with 1000 W/M² Irradiation

Adding the PV to the system has increased the load RMS voltage. It is also clear that the controller of ANFIS and ANN modulated by SPWM produces the quickest response to the reference point as shown in "Fig. 8".

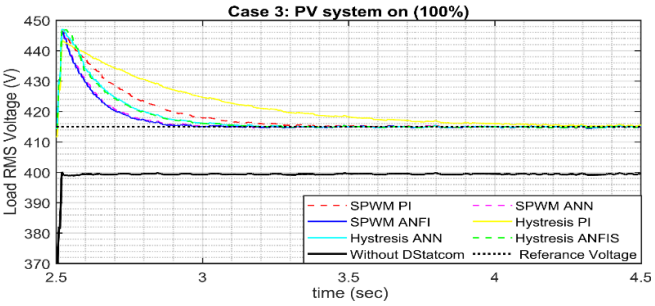

Fig. 8. RMS voltage of load while PV active.

From "Table 5." the ANFIS controller using SPWM has the smallest RMSE, settling time, and rising time. Its settling average value is the highest. The Hysteresis-using ANN controller, in contrast to the other controllers, has a lower SSError value.

D. Scenario 4: Two-Phase to Ground Fault on The System

"Fig. 9" shows the load RMS voltage graph has been corrected to reference voltage (415V) when the ABG fault is applied in the power system.

From "Table 6." the ANFIS controller using SPWM has the smallest RMSE, settling time, and rising time. Its settling average value is the highest. On the other hand, the controller of the PI with Hysteresis has the lowest settling time and rise time. Also, it achieved the best Settling Average Value compared to other controllers.

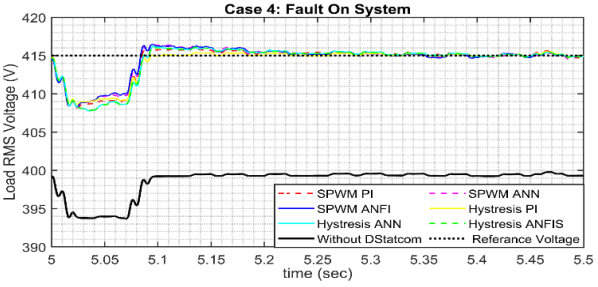

Fig. 9. RMS voltage during an ABG fault condition.

However, other controllers' performance was not effective in case of ABG fault active, and only the SPWM ANFIS has shown better RSME and SSError. In this case, the performance of the Hysteresis PI controller was better in settling time, settling average value, and rise time.

Table 3. Performance evaluation of the results during 1-2s when D-STATCOM is active

D-STATCOM ON						
Hisit_ANN	Hisit_PI	SPWM_PI	Hisit_ANN	Hisit_ANFIS	SPWN_ANN	SPWN_ANFIS
RMSE	6.36%	5.30%	5.48%	5.40%	5.02%	5.00%
SSError	0.9099	0.603	0.5403	0.4228	0.102	0.2173
Settling Time (ms)	167.388	114.377	66.563	73.868	66.664	65.312
Settling Avg. value	413.047	414.009	413.649	413.698	414.332	414.01
Rise Time (ms)	448.736	242.715	176.536	182.014	142.554	120.294
Peak	414.154	415.397	414.981	415.007	415.765	415.367

Table 4. Simulation results for 2-2.5s when additional load is active

Additional load On						
	Hisit_PI	SPWM_PI	Hisit_ANN	Hisit_ANFIS	SPWN_ANN	SPWN_ANFIS
RMSE	5.52%	3.61%	3.47%	3.46%	2.41%	2.30%
SSError	3.2424	0.5676	0.5379	0.319	0.2761	0.3761
Settling Time (ms)	363.485	358.228	295.507	287.745	393.773	244.769
Settling Avg. value	409.956	410.798	410.908	414.697	411.625	415.21
Rise Time (ms)	1514.35	704.784	544.447	623.955	607.911	395.906
Peak	414.21	415.056	414.478	414.721	415.472	415.47

Table 5. Performance evaluation of results during 2.5-4.5s when PV is active

PV on 100%						
	Hisit_PI	SPWM_PI	Hisit_ANN	Hisit_ANFIS	SPWN_ANN	SPWN_ANFIS
RMSE	11.21%	8.64%	7.80%	7.80%	6.34%	6.17%
SSError	1.0292	0.0951	0.0418	0.0756	0.0832	0.077
Settling Time (ms)	893.602	475.931	361.889	354.85	257.025	252.001
Settling Avg value	429.718	430.744	430.947	431.055	430.466	429.057
Rise Time (ms)	947.992	858.923	812.672	579.379	565.054	472.563
Peak	443.608	446.758	447.177	447.423	446.4	446.233

Table 6. Performance evaluation of results during 5-5.5s while fault is active

Two-phase to ground fault						
	Hisit_PI	SPWM_PI	Hisit_ANN	Hisit_ANFIS	SPWN_ANN	SPWN_ANFIS
RMSE	2.13%	2.25%	2.40%	2.39%	2.13%	2.09%
SSError	0.0962	0.2212	0.1565	0.1263	0.2168	0.0904
Settling Time (ms)	90.834	471.603	267.457	216.604	273.025	266.055
Settling Avg value	415.175	412.031	415.493	415.474	415.572	415.551
Rise Time (ms)	0.363	0.372	0.445	0.372	0.386	0.39
Peak	415.513	415.906	416.248	416.172	416.612	416.479

Table 7. Performance evaluation of results during 6-8 WHEN PV POWER DROPS TO 50%

PV on 50%						
	Hisit_PI	SPWM_PI	Hisit_ANN	Hisit_ANFIS	SPWN_ANN	SPWN_ANFIS
RMSE	16.53%	11.57%	9.99%	9.93%	8.10%	7.87%
SSError	4.3148	0.2677	0.8114	0.1177	0.0509	0.104
Settling Time (ms)	776.749	525.932	445.17	457.214	330.66	327.821
Settling Avg value	396.451	414.671	400.313	414.841	415.05	415.155
Rise Time (ms)	719.182	706.406	664.967	682.463	626.384	179.882
Peak	414.745	414.867	414.882	415.287	415.506	415.632

Table 8. Performance evaluation of results during 8-10s with disconnection of additional load

Additional load Off						
	Hisit_PI	SPWM_PI	Hisit_ANN	Hisit_ANFIS	SPWN_ANN	SPWN_ANFIS
RMSE	3.28%	2.69%	3.12%	2.72%	1.98%	1.91%
SSError	0.7337	0.2467	0.1751	0.0651	0.1751	0.0656
Settling Time (ms)	626.083	436.496	452.464	272.129	255.502	254.916
Settling Avg value	419.353	419.342	419.464	414.921	419.093	419.174
Rise Time (ms)	1514.35	704.784	544.447	623.955	607.911	395.906
Peak	423.534	424.167	424.238	424.361	423.808	423.768

Table 9. Performance evaluation of results during 10-11s while PV power increased to 80%

PV On to 80%						
	Hisit_PI	SPWM_PI	Hisit_ANN	Hisit_ANFIS	SPWN_ANN	SPWN_ANFIS
RMSE	6.96%	5.08%	5.06%	4.44%	3.60%	3.49%
SSError	1.4215	0.0818	0.0824	0.073	0.0618	0.0492
Settling Time (ms)	774.759	531.192	282.371	352.724	271.763	271.757
Settling Avg value	422.886	422.05	422.464	422.19	421.614	421.437
Rise Time (ms)	1097.09	836.779	826.993	775.717	850.257	704.364
Peak	429.515	429.479	430.355	429.795	428.922	428.424

E. Scenario 5: PV Drops To 50%

In this scenario, the PV system power is reduced to 50 % due the drop in the irradiation to 500 (W/m2) over the time (6 to10) s of the simulation time.

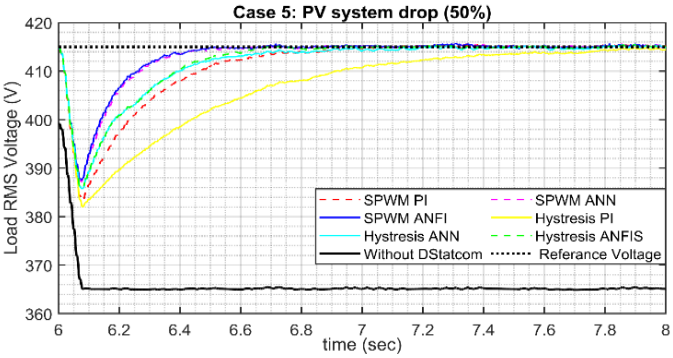

Fig. 10. RMS voltage when PV power drops to 50%.

It can be noticed from "Fig. 10" that the controllers have corrected the load RMS voltage to the reference voltage (415V) once the PV power drops due to the irradiation effects. From" Table 7." the ANFIS controller using SPWM has the smallest RMSE, SSError, settling time, and rising time. Meanwhile the SPWM-using ANN controller, has the best Settling Average Value.

F. Scenario 6: The Additional Load Disconnected

"Fig. 11" show that the voltage has been adjusted to the reference voltage (415V) after the load is disconnected from the power system.

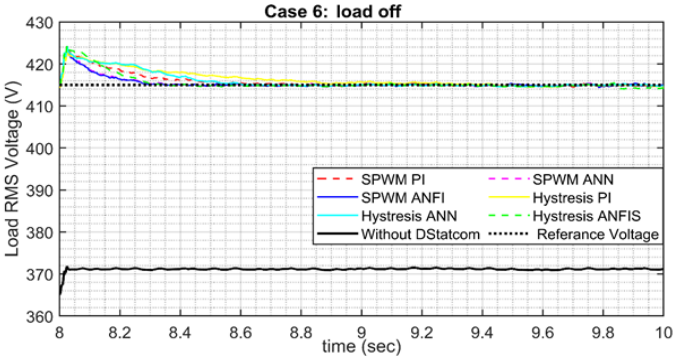

Fig.11. RMS voltage when disconnecting the added load.

From "Table 8." the ANFIS controller using SPWM has the lowest RMSE, SSError, settling time, and rising time. And he Hysteresis -using ANN controller, has the best Settling Average Value.

G. Scenario 7: PV Increases To 80%

In this scenario, the PV system power is increased to 80 % increasing the irradiation to 800 (W/m2) over time (10 to11) s of the simulation time.

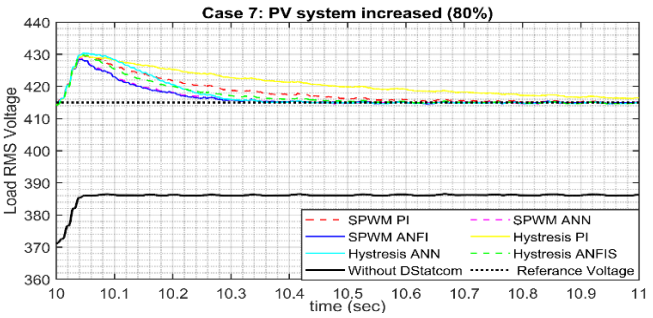

Fig. 12. RMS voltage when PV power is increase to 80%.

It can be noticed from "Fig. 12" that the D-STATCOM corrects the load RMS voltage to the reference voltage (415V) despite the PV power is increased to 80%. From "Table 9." the ANFIS controller using SPWM has the lowest RMSE, SSError, settling time, and rising time the best Settling.

H. Scenario 8: PV Off

The PV system is disconnected from the main power system at 11 s, the simulation time in this scenario. It can be noticed from "Fig. 13" The load RMS voltage is corrected by the D-STATCOM action to the reference voltage (415V) despite disconnecting the PV from the system.

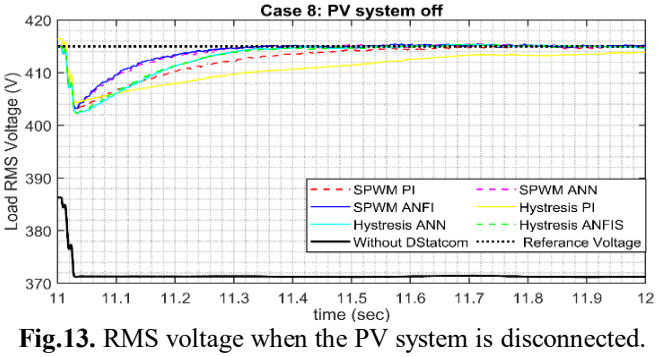

Fig.13. RMS voltage when the PV system is disconnected.

From "Table 10." the ANFIS controller using SPWM has the smallest RMSE, settling time, rising time the best Settling Average Value. However, the SPWM-using ANN controller, has the lowest SSError.

Table 10. Performance evaluation of results during 11-12s while PV system is disconnected

PV System disconnected						
	Hisit_PI	SPWM_PI	Hisit_ANN	Hisit_ANFIS	SPWN_ANN	SPWN_ANFIS
RMSE	4.85%	3.82%	3.81%	3.71%	2.78%	2.70%
SSError	1.0885	0.106	0.3099	0.2773	0.0643	0.1835
Settling Time (ms)	654.519	441.472	274.732	277.43	263.822	245.899
Settling Avg value	409.13	414.889	408.804	408.799	409.322	415.113
Rise Time (ms)	1124.43	701.865	897.449	773.265	534.085	402.271
Peak	416.554	415.263	415.341	415.369	415.533	415.554

I. Total Harmonic Distortion (THD)

"Table 11." of the specific THD results for the total harmonic distortion of the voltage for the SPWM- (ANN, and ANFIS) and Hysteresis- (ANN, and ANFIS).

The SPWM with the ANFIS controls technique had the lowest THD percentage of 1.64 as shown in "Fig. 14". While the D-STATCOM-based system with the PI Hysteresis controller had a maximum THD of 1.95% as shown in "Fig. 15". When there was no external controller present in the system, THD was approximately 3.57%.

Table 11. Comparison of THD for different controllers

	PI	**ANN**	**ANFIS**	**Without D-STATCOM**
Hysteresis	1.95%	1.75%	1.76%	3.57%
SPWM	1.78%	1.65%	1.64%	3.57%

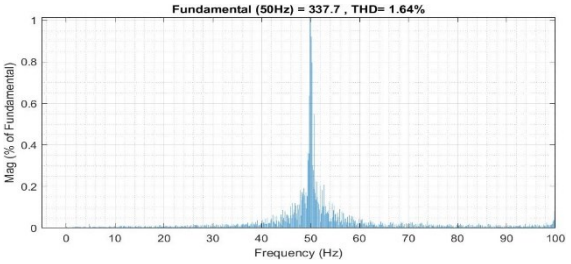

Fig. 14. THD in voltage for ANFIS-SPWM.

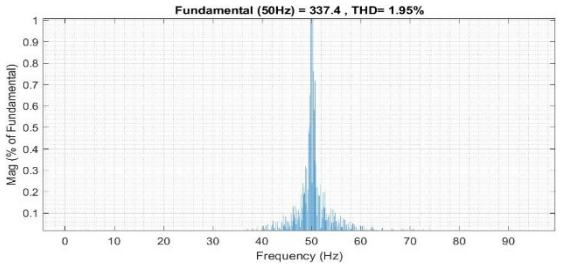

Fig. 15. THD in voltage for PI- Hysteresis.

7. Conclusion

In conclusion, The ANFIS controller using SPWM invertor indicated from the resalt has a best control than other control methods. The SPWM inverter technique was thus found to adjust the control input more quickly than the Hysteresis scheme.

The controller of ANFIS and ANN-based D-STATCOM can mitigate power quality problems related to PV integration to reduce the adverse impact of the PV integration on voltage regulation and harmonic distortion.

Where the main findings of the simulation analysis demonstrates that ANFIS SPWM D-STATCOM, achieves the smoothness of the load voltage profile, the lowest RMSE, and the quickest control response. This demonstrates the powerful control of ANFIS, a system that models and controls ill-defined and unpredictable systems using an intelligent Neuro-Fuzzy method. However, the SPWM ANN control scheme for D-STATCOM, however, performs better than other control schemes in a few scenarios because it has the lowest steady-state error (SSError) in scenarios 2 (attach new load) and 8. (disconnected PV system).

Meanwhile In Scenario 4 (fault state), which is the most dangerous scenario in all cases because an external disturbance is applied to the system, has the lowest settling time and rising time for the Hysteresis PI control scheme. This may be explained by the controller's slow response following a fault in the system, which allows it to maintain the system's voltage profile without having a rapid reaction time that could distort the system. Finally, the THD was calculated using the voltage profile, and the results show that the controller ANFIS using SPWM has the lowest value of THD in the system as shown in "Table 11."

The performance of SPWM with ANFIS was better than other control schemes in most scenarios. Hence, it was found that the SPWM inverter strategy adapts the control input faster than the Hysteresis scheme. The above conclusion signifies that the performance of advanced controllers, especially ANFIS, which has an intelligent Neuro-Fuzzy technique used for modeling and controlling ill-defined and uncertain systems, was better controller among other controllers. It can effectively enhance the power quality of the power system using D-STATCOM devices.

8. Future Recommendation

This research motivates further investigation of new and modern algorithms such as Adaptive Neuro-Fuzzy Takagi-Sugeno-Kang (ANFTSK), Adaptive Neuro-Fuzzy Wavelet (ANFW), and Typ-2 ANF controllers. Further research will focus on the performance of these advanced control techniques when integrated with FACTS devices to enhance voltage profile, improve power quality and reduce THD in voltage and current profiles. Similarly, finding the optimal parameters of a control technique at which D-FACTS devices perform at their best is a crucial aspect of future research. Furthermore, the integration of Wind power systems can also bring its limitations into the power system, and the research can be extended by incorporating wind and PV integrated power systems.

References

[1] N. Khan, S. Dilshad, R. Khalid, A. R. Kalair, and N. Abas, "Review of energy storage and transportation of energy," Energy Storage, vol. 1, no. 3, p. e49, Jun. 2019, doi: https://doi.org/10.1002/est2.49.

[2] A. R. Gidd, A. D. Gore, S. B. Jondhale, O. V. Kadekar, and M. P. Thakre, "Modelling, analysis and performance of a DSTATCOM for voltage Sag mitigation in distribution network," in 2019 3rd International Conference on Trends in Electronics and Informatics (ICOEI), 2019, pp. 366–371. doi: 10.1109/ICOEI.2019.8862554.

[3] E. Mostafa and N. K. Bahgaat, "A comparison between using a firefly algorithm and a modified PSO technique for stability analysis of a PV system connected to grid," International Journal of Smart Grid, 2017, [Online]. Available: https://api.semanticscholar.org/CorpusID:67121814

[4] Y. Abdelkader, T. Allaoui, and C. Abdelkader, "Power quality improvement based on five-level shunt APF using sliding mode control scheme connected to a photovoltaic," International Journal of Smart Grid, 2017, [Online]. Available: https://api.semanticscholar.org/CorpusID:67443390

[5] D. Rekioua, K. Kakouche, P.-O. Logerais, and T. Rekioua, "Power control-based fuzzy and modulated hysteresis methods for micro-grid using a photovoltaic system," in 2023 11th International Conference on Smart Grid (icSmartGrid), 2023, pp. 1–6. doi: 10.1109/icSmartGrid58556.2023.10170869.

[6] M. A. Basit, S. Dilshad, R. Badar, and S. M. Sami ur Rehman, "Limitations, challenges, and solution approaches in grid-connected renewable energy systems," Int J Energy Res, vol. 44, no. 6, pp. 4132–4162, May 2020, doi: https://doi.org/10.1002/er.5033.

[7] J. O. Petinrin and M. Shaaban, "Impact of renewable generation on voltage control in distribution systems," Renewable and Sustainable Energy Reviews, vol. 65, pp. 770–783, 2016, doi: https://doi.org/10.1016/j.rser.2016.06.073.

[8] T. M. Blooming and D. J. Carnovale, "Application of IEEE std 519-1992 harmonic limits," in Conference record Of 2006 Annual Pulp and Paper Industry Technical Conference, IEEE, 1992, pp. 1–9. doi: 10.1109/PAPCON.2006.1673767.

[9] E. Hossain, M. R. Tür, S. Padmanaban, S. Ay, and I. Khan, "Analysis and mitigation of power quality issues in distributed generation systems using custom power devices," IEEE Access, vol. 6, pp. 16816–16833, 2018, doi: 10.1109/ACCESS.2018.2814981.

[10] W. Rohouma, R. S. Balog, M. M. Begovic, and A. A. Peerzada, "Use of D-STATCOM for solid state LED lamp harmonic power mitigation," in 2022 10th International Conference on Smart Grid (icSmartGrid), 2022, pp. 149–154. doi: 10.1109/icSmartGrid55722.2022.9848763.

[11] W. Rohouma, M. Metry, R. S. Balog, A. A. Peerzada, M. M. Begovic, and D. Zhou, "Analysis of the capacitor-less D-STATCOM for voltage profile improvement in distribution network with high PV penetration," IEEE Open Journal of Power Electronics, vol. 3, pp. 255–270, 2022, doi: 10.1109/OJPEL.2022.3167548.

[12] E. S. Oda, A. M. A. el Hamed, A. Ali, A. A. Elbaset, M. A. el Sattar, and M. Ebeed, "Stochastic optimal planning of distribution system considering integrated photovoltaic-based DG and DSTATCOM under uncertainties of loads and solar irradiance," IEEE Access, vol. 9, pp. 26541–26555, 2021, doi: 10.1109/ACCESS.2021.3058589.

[13] K. R. Sree Jyothi, P. Venkatesh Kumar, and J. JayaKumar, "A review of different configurations and control techniques for DSTATCOM in the distribution system," E3S Web of Conferences, vol. 309, p. 1119, Oct. 2021, doi: 10.1051/e3sconf/202130901119.

[14] B. Singh, P. Jayaprakash, and D. P. Kothari, "New control approach for capacitor supported DSTATCOM in three-phase four wire distribution system under non-ideal supply voltage conditions based on synchronous

reference frame theory," International Journal of Electrical Power & Energy Systems, vol. 33, no. 5, pp. 1109–1117, Jun. 2011, doi: 10.1016/j.ijepes.2010.12.006.

[15] A. J. Rana, C. K. Vasoya, M. H. Pandya, and P. M. Saradva, "Application of unit template algorithm for voltage sag mitigation in distribution line using D-STATCOM," in 2016 International Conference on Energy Efficient Technologies for Sustainability (ICEETS), IEEE, Apr. 2016, pp. 756–761. doi: 10.1109/ICEETS.2016.7583849.

[16] B. Singh and S. Kumar, "Modified power balance theory for control of DSTATCOM," in 2010 International Conference on Power Electronics, Drives and Energy Systems & 2010 Power India, IEEE, Dec. 2010, pp. 1–8. doi: 10.1109/PEDES.2010.5712547.

[17] M. Deben Singh, R. K. Mehta, and A. K. Singh, "Integrated fuzzy-PI controlled current source converter-based D-STATCOM," Cogent Eng, vol. 3, no. 1, p. 1138921, Dec. 2016, doi: 10.1080/23311916.2016.1138921.

[18] B. Ersöz, Ş. Sağıroğlu, and H. İ. Bülbül, "A short review on explainable artificial intelligence in renewable energy and resources," in 2022 11th International Conference on Renewable Energy Research and Application (ICRERA), 2022, pp. 247–252. doi: 10.1109/ICRERA55966.2022.9922870.

[19] V. Ponananthi and B. R. Kumar, "Three-phase statcom controller using D-Q frame theory for a three-phase SEIG feeding single phase loads," in 2nd International Conference on Electronics and Communication Systems, ICECS 2015, Institute of Electrical and Electronics Engineers Inc., Jun. 2015, pp. 926–931. doi: 10.1109/ECS.2015.7125050.

[20] Cheol-Taek Kim and Ju-Jang Lee, "Training two-layered feedforward networks with variable projection method," IEEE Trans Neural Netw, vol. 19, no. 2, pp. 371–375, Feb. 2008, doi: 10.1109/TNN.2007.911739.

[21] D. Karaboga and E. Kaya, "Adaptive network based fuzzy inference system (ANFIS) training approaches: a comprehensive survey," Artif Intell Rev, vol. 52, no. 4, pp. 2263–2293, Dec. 2019, doi: 10.1007/s10462-017-9610-2.

[22] K. D. E. Kerrouche, E. Lodhi, M. B. Kerrouche, L. Wang, F. Zhu, and G. Xiong, "Modeling and design of the improved D-STATCOM control for power distribution grid," SN Appl Sci, vol. 2, no. 9, p. 1519, 2020, doi: 10.1007/s42452-020-03315-8.

[23] V. 0 Application Note, "Setting the P-I Controller Parameters, KP and KI Application Note TLE7242 and TLE8242 Automotive Power," 2009.